17 Apr 2004, 10:30am - 12:30pm

Nonlinear Dynamic Behavior of Pile Groups: Effects of Plasticity of Soil

B. K. Maheshwari
Birla Institute of Technology & Science, Pilani, Rajasthan, India

Kevin Z. Truman
Washington University, St. Louis, Missouri


Proceedings: Fifth International Conference on Case Histories in Geotechnical Engineering
New York, NY, April 13-17, 2004

NONLINEAR DYNAMIC BEHAVIOR OF PILE GROUPS: EFFECTS OF PLASTICITY OF SOIL

B.K. Maheshwari
Civil Engineering Group
Birla Institute of Technology & Science
Pilani, Rajasthan 333 031, India

Kevin Z. Truman
Dept. of Civil Engineering
Washington University
St. Louis, MO 63130, USA

ABSTRACT

The effects of material nonlinearity of soil on dynamic behavior of a single pile and pile groups are investigated. An advanced plasticity based soil model, HiSS, is incorporated in the finite element formulation. To simulate radiation effects, proper boundary conditions are used. The model and algorithm are verified with analytical results that are available for elastic and elasto-plastic soil models. Analyses are performed for seismic excitation as well as for loads applied on the pile cap and the effect of nonlinearity is investigated. Effects of spacing between piles are investigated. It was found that the effect of soil nonlinearity on the seismic response is very much dependent on the frequency of excitation. At low frequencies, its effect is significant but at higher frequencies it is negligible. For the loading on a pile cap, the nonlinearity decreases the dynamic stiffness of the soil-pile system. Effect of nonlinearity on the dynamic stiffness is shown to be sensitive to the spacing between piles. Nonlinearity suppresses wave interference effects among piles and thus reduces the stiffness significantly at excitation frequencies where the group effect is most important.

INTRODUCTION

Much of the reported research for dynamic analysis of pile foundations assumes linear behavior of the soil media. Kaynia and Kausel (1982), Sen et al. (1985), Dobry and Gazetas (1988), and Makris and Gazetas (1992) among others have investigated the dynamic response of pile groups assuming linear soil behavior. However, under strong seismic excitation, the nonlinear behavior of the soil media has a strong influence on the response of the pile foundation. Foundation failures during recent devastating earthquakes (e.g. Bhuj Earthquake of 2001, Chi-Chi Earthquake of 1999, and Kocaeli Earthquake of 1999) have shown that nonlinearity should be taken into account when designing pile foundations.

The response analysis should be performed in the time domain to properly account for the soil nonlinearity. Therefore, the focus in recent years has shifted to incorporate the nonlinear behavior of soil media using time domain analyses. Nogami and Konagai (1986, 1988) analyzed the dynamic response of pile foundations in the time domain analysis using a Winkler approach. Nogami et al. (1992) introduced material and geometrical nonlinearity in the analysis using discrete systems of mass, spring and dashpots.

It is difficult to properly represent damping and inertia effects of continuous, semi-infinite soil media when using such systems. Further, full coupling in the axial and lateral directions may not be considered. Inclusion of material nonlinearity caused by the plasticity of the soil demands that an analysis be performed in real time using finite elements to adequately represent possible inhomogeneous soil media. Using strain dependent moduli and damping, and a tension cutoff, Wu and Finn (1997) presented a quasi-3D method for nonlinear dynamic analysis. Bentley and El Naggar (2000) investigated the kinematic response of single piles to account for the soil plasticity using the Drucker-Prager soil model, and gapping at the soil-pile interface. However, they did not consider work hardening of the soil media. Attempts were made by Cai et al. (2000) to include the plasticity and work hardening of soil using a finite element technique in the time domain. However they assumed fixed boundary conditions and neglected damping in the foundation subsystem. Also in that analysis the effects of plasticity has not been investigated.

Using the HiSS (hierarchical single surface) soil model, Maheshwari et al. (2002) examined the effects of plasticity and work hardening of soil on the free field response as well as on the kinematic response of single piles. In this paper, the model is extended and analyses were performed to study the dynamic behavior of pile groups.

FINITE ELEMENT MODEL

Full three-dimensional geometric models were used to represent the soil-pile systems. Taking advantage of symmetry and anti-symmetry (as shown in Fig. 3a) only one fourth of the actual model was built, thus dramatically improving efficiency of computation. Finite element quarter models of a single pile and 2*2 pile groups are shown in Figs. 1a-d.

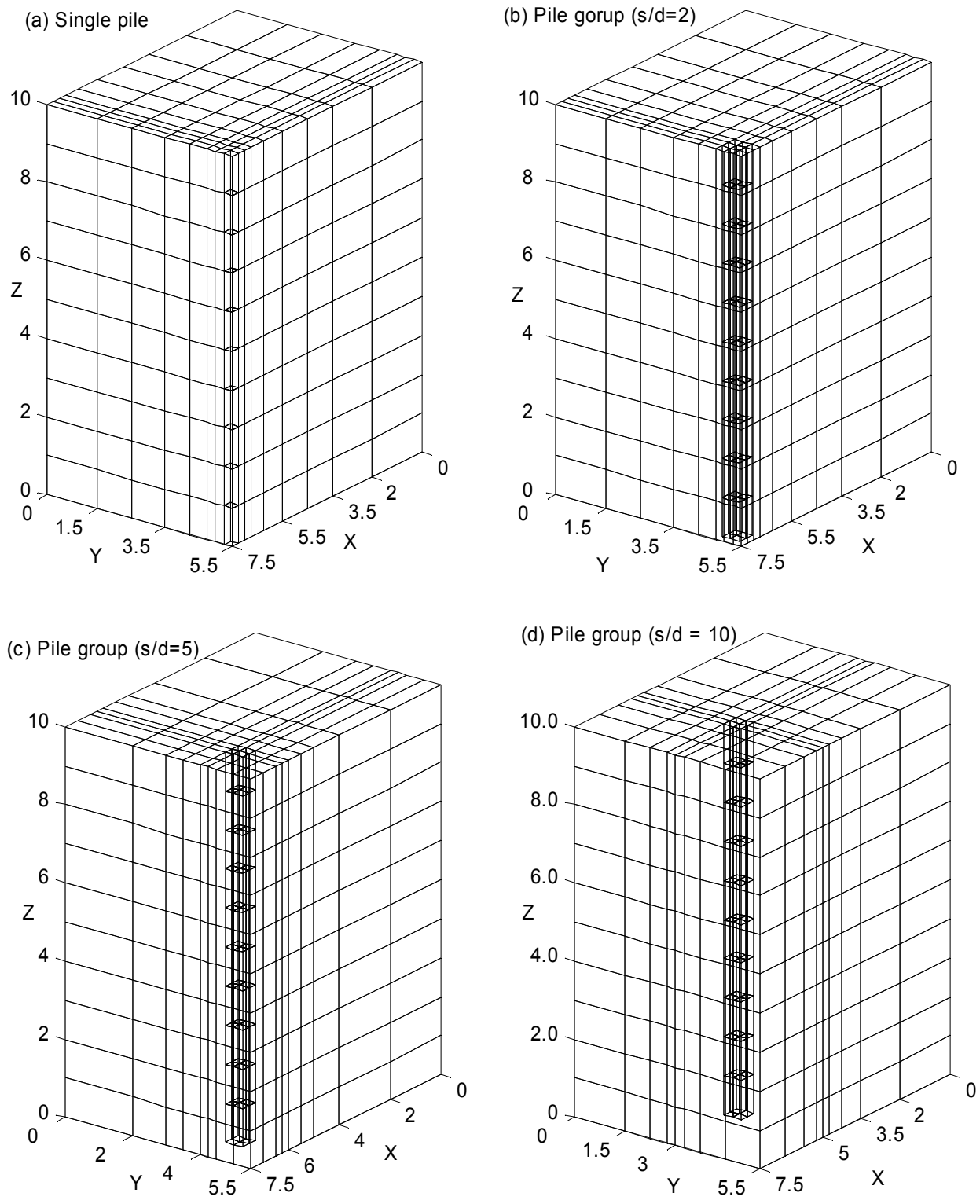

Fig. 1. Three-dimensional finite element meshes for the soil-pile system: (a) single pile, (b) pile group (s/d = 2), (c) pile group (s/d = 5), (d) pile group (s/d = 10).

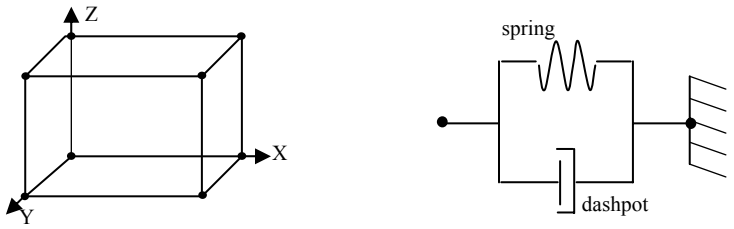

(a) 8-noded Block Element (b) 2-noded Boundary Element

Fig. 2. (a) Block element used for soil and pile, (b) Boundary element (spring and dashpot).

All piles have a square cross-section, d*d. The piles are fully embedded in the soil and are socketed in the bedrock. For the pile groups, three pile spacing (centre-to-centre) ratios s/d = 2, 5 and 10 were considered. The mesh size, number of elements and number of nodes used in all four models are exactly the same.

The soil and piles are modeled using eight-node hexahedral elements. Each node has three translational degrees of freedom, i.e. in the X, Y and Z coordinate directions as shown in Fig. 2a. To simulate an infinite soil medium, Kelvin elements (spring and dashpot as shown in Fig. 2b) are attached in all three directions (i.e. X, Y and Z) along the mesh boundaries in order to model the far field conditions and allow for wave propagation. The coefficients of the springs and dashpots are derived separately for the horizontal and vertical directions as will be discussed below.

For all models, elements are kept very small near the pile(s) and gradually increase in size moving away from the pile(s). For example, the details of the finite element mesh in plan and elevation for the case of s/d = 5 are shown in Fig. 3. The size of the elements near the pile is kept less than one sixth of the wave-length that corresponds to the highest frequency of 20 Hz considered in the analysis (Kramer 1996). The mesh was refined near the pile to account for the severe stress gradients and plasticity encountered in the soil. Specifications for the mesh are: size in plan 7.5 m × 5.5 m and a height of 10 m. In plan, the size of the elements varies from 0.25 m to 2 m while the element size is kept uniform at 1m in the vertical direction to allow for an even distribution of vertically propagating SH waves. A total of 720 elements were used in the model.

For pile groups, a rigid massless pile cap connects all pile-heads. Pile elements are assumed to behave linearly but they can also be nonlinear by using an appropriate constitutive relation. For the nonlinear soil model (HiSS), the initial stress condition in the soil is governed by the confining pressure of the soil and is proportional to the depth (Fig. 3b). The seismic excitation is assumed to act on the fixed base nodes and is assumed to consist of vertically propagating shear waves. Since the analysis is in the time domain, a complete three-dimensional excitation can be used.

FORMULATION AND PROCESS OF ANALYSES

Governing Equation and Solution

The load is considered to be transient and represented by a digitized load time history. The governing equation of motion at time $t+\Delta t$, is:

$$M\,{}^{t+\Delta t}\ddot{U} + C\,{}^{t+\Delta t}\dot{U} + K\,{}^{t+\Delta t}U = {}^{t+\Delta t}R \qquad (1)$$

M is a diagonal mass matrix because all masses are lumped at the nodal points. C is a global damping matrix that includes the effects of both material damping and radiation damping (including dashpots along the boundary). K is a symmetric stiffness matrix determined assuming full coupling in all three directions of motion and includes the stiffness of springs at the boundary nodes. The external load at time step $t+\Delta t$ is ${}^{t+\Delta t}R$. Finally, U, $\dot{U}$ and $\ddot{U}$ are relative nodal displacement, velocity and acceleration, respectively at time $t+\Delta t$. Employing the constant average acceleration method of integration (Bathe 1982), Eq. (1) is solved for displacement ${}^{t+\Delta t}U$.

For the linear case, the analysis is carried incrementally but stiffness and damping matrices remain constant throughout the analysis and no iterative procedure is required. When soil plasticity is included, matrices K and C do not remain constant but change after each time step. Therefore, Modified Newton-Raphson iterative scheme is used for the solution.

Boundary Conditions

Kelvin elements are used at the boundary, as shown in Figs. 3a and 3b. The presence of the springs provides stiffness, giving this boundary a distinct advantage over the standard viscous boundary (Wolf 1985, Novak and Mitwally 1988). To evaluate the constants of spring and dashpot for transient excitation, predominant frequency of excitation (derived from corresponding Fourier spectrum) is used.

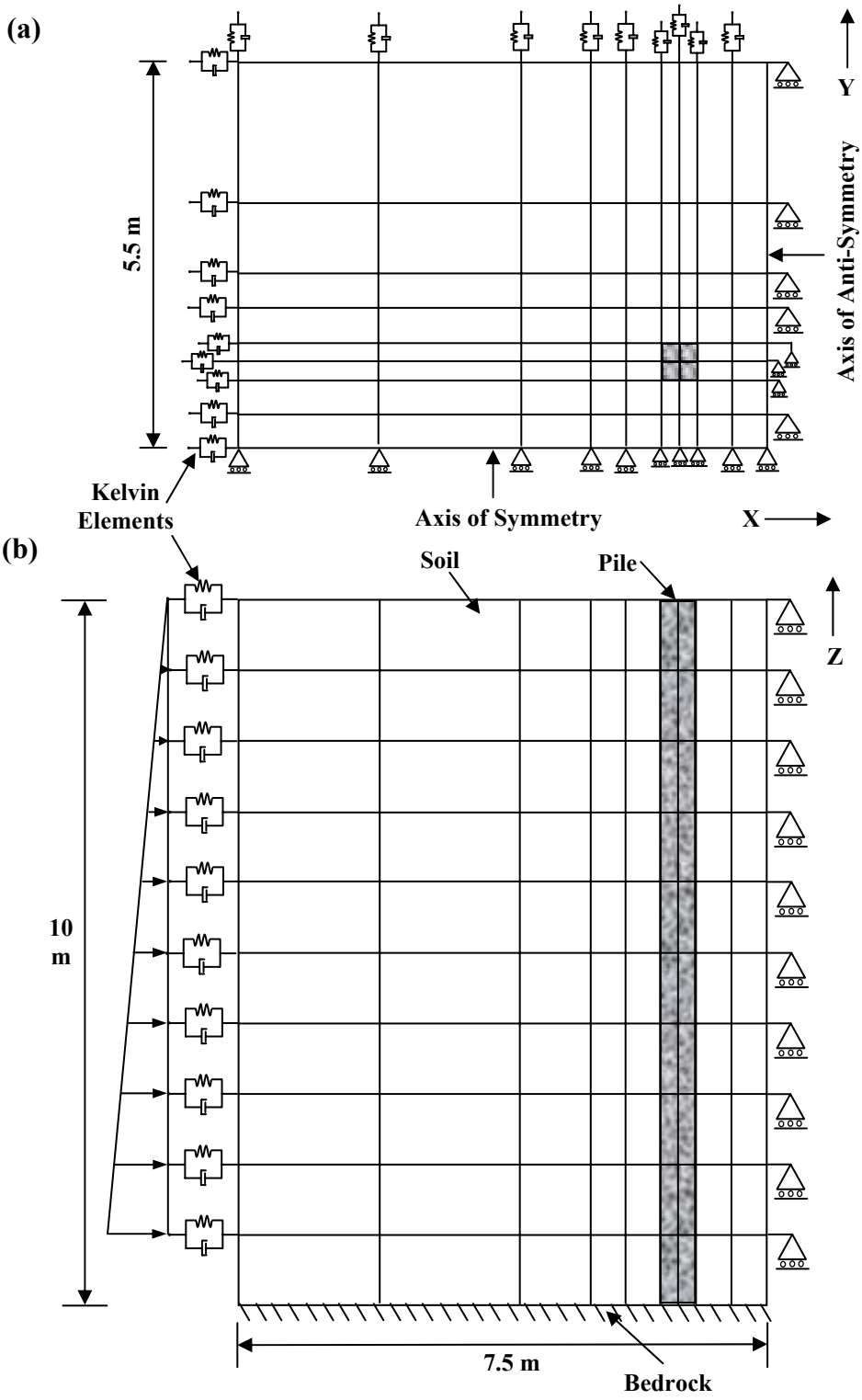

Fig. 3. Finite element mesh with boundary conditions for 2*2 pile group (s/d = 5): (a) Top plan (b) Front elevation with initial pressure distribution

The constants of the spring and dashpot of the Kelvin element in the two horizontal directions were calculated using the solution developed by Novak and Mitwally (1988) and is given by:

$$k_r^* = \frac{G}{r_0}[S_1(a_r, \upsilon, D) + iS_2(a_r, \upsilon, D)] \quad (2a)$$

where k_r^* is the complex stiffness, G is the shear modulus of soil, r_0 is distance in plan (Fig. 3a) from the center of the foundation to the node where Kelvin element is attached. S_1 and S_2 are the dimensionless parameters from closed-form solutions, D is the material damping ratio, ν is Poisson's ratio and i is the imaginary unit = $\sqrt{-1}$. Finally, a_r is the dimensionless frequency = $r_0\omega/V_s$, where ω is the angular frequency of excitation and V_s is the shear wave velocity of the soil. The real and imaginary parts of Eq. (2a) represent the stiffness and damping, respectively, i.e.

$$k_r = \frac{GS_1}{r_0} \quad and \quad c_r = \frac{GS_2}{\omega r_0} \quad (2b)$$

The damping term vanishes for the static case and the element reduces to a spring only. Similarly, the constants for the vertical direction are given by (assuming plane strain conditions) (Novak et al. 1978):

$$k_w^* = \frac{G}{r_0}[S_{w1}(a_r, D) + iS_{w2}(a_r, D)] \quad (3a)$$

where the subscript w is used to represent the vertical direction and the other parameters are the same as in Eq. (2a). Stiffness and damping for the vertical direction are determined in a similar fashion to Eq. (2b), i.e.

$$k_w = \frac{GS_{w1}}{r_0} \quad and \quad c_w = \frac{GS_{w2}}{\omega r_0} \quad (3b)$$

To determine the stiffness and damping of the Kelvin elements, the constants, given by Eqs. (2b) and (3b) are multiplied by the area of the element face (normal to the direction of loading). It should be noted that stiffness and damping arising due to Kelvin elements on the boundary area are lumped while those arising due to finite elements in this area are consistent. Also, for the vertical direction the dimensionless parameters S_{w1} and S_{w2} are independent of Poisson's ratio and for the static case both the spring and dashpot terms vanish. Thus, for the low frequency range the spring and dashpot constants are adjusted to match more rigorous solutions by choosing a minimum cutoff frequency (a_r = 0.3) below which the stiffness is taken as constant (=2) and the damping is taken as linear.

The nodes on the axis of symmetry are free to move in the vertical direction and along the direction of the axis of symmetry, and are fixed in the perpendicular horizontal direction (Fig. 3a). The nodes on the axis of anti-symmetry are constrained in the direction of this axis and vertical direction while free to move in the perpendicular horizontal direction (Figs. 3a and 3b). All the nodes along the base are fixed in all three directions (Fig. 3b).

Damping Matrix (C)

To adequately represent damping in the system, both radiation and material damping are considered in the analysis. Thus, the damping matrix C consists of two parts, radiation damping C_r and material damping C_m, i.e.

$$C = C_r + C_m \quad (4a)$$

Radiation damping C_r is a diagonal matrix and has non-zero terms only at the nodes on the boundary where Kelvin elements are attached. Damping coefficients for the dashpots in the horizontal and vertical directions are calculated using Eqs. (2b) and (3b), respectively. For conceptual and computation reasons (Guin & Banerjee, 1998), material damping C_m is taken as proportional to stiffness and is given by:

$$C_m = \alpha K \quad \text{where} \quad \alpha = 2D/\omega_0 \quad (4b)$$

where D is the material damping ratio and ω_0 is the predominant circular frequency of loading.

Pile Cap

For pile groups, it was assumed that a rigid massless cap connects all the pile heads. Therefore deformations of all pile heads would be the same as that of the cap. Also, force compatibility is enforced between the pile heads and the cap to maintain equilibrium. The formulation and algorithm is modified accordingly to account for the effect of the pile cap. The rigid pile cap requires the displacements in all pile heads to be equal to that in the cap but introduces additional external unknown forces to be transferred from the cap to pile heads. To solve Eq. (1) in the case of a rigid pile cap, the matrices are condensed in terms of the nodes at pile heads. This condensation is performed keeping intact the skyline form of the matrices without developing full matrices to maintain the efficiency in computation (Felippa 1975).

After completion of matrix condensation, the force-displacement relationship is transferred to a specified point on the cap (centroid of the cap in the present analysis) using a compatibility matrix L between the pile head and pile cap. Forces and displacements in the pile cap are related to those at the pile heads as:

$$P_c = L^T P_h \quad and \quad U_h = LU_c \quad (5)$$

where subscripts c and h stand for the pile cap and pile heads, respectively. L^T is the transpose of the matrix L. It is noted that

the compatibility matrix L depends only on the geometry of the cap and type of connection. For a rigid massless cap assumed here, all non-zero elements of L will be unity. To deal with a hinge connection one has to change the matrix L only.

Finally, by solving the force-displacement relationship at the pile cap, the displacement of pile cap is found. The displacements at the pile heads and other nodes are found through back substitution, which concludes computation for a specific time step. The process is repeated at every time step. Furthermore, for seismic analysis the condition that the resultant of the pile head forces on the pile cap is zero must be satisfied.

HiSS Soil Model

A nonlinear soil model HiSS has been used to introduce the effect of plasticity. There is a series of these models, as mentioned in Wathugala and Desai (1993). In the present work, the δ_0^* version of HiSS is considered. Both plasticity and work hardening of the soil are considered in the model, which is based on an incremental stress-strain relationship and assumes associative plasticity. Further, this version assumes the constitutive relationship for nonvirgin loading (i.e. loading or unloading) to be elastic. A simplified formulation used for virgin loading in HiSS is described here. Further details can be found in Wathugala and Desai (1993).

In this model, a material parameter, β, is used to define the shape of the yield surface in the octahedral plane. Assuming $\beta=0$, the dimensionless yield surface F can be simplified as:

$$F=\left(\frac{J_{2D}}{p_a^2}\right)+\alpha_{ps}\left(\frac{J_1}{p_a}\right)^{\eta}-\gamma\left(\frac{J_1}{p_a}\right)^{2}=0 \qquad (6a)$$

where J_1 is the first invariant of the stress tensor σ_{ij}; J_{2D} is the second invariant of the deviatoric stress tensor; p_a is the atmospheric pressure; γ and η are material parameters that influence the shape of F in J_1-$\sqrt{J_{2D}}$ space; parameter η is related to the phase change point that is defined as the point where material changes from contractive to dilative behavior (Fig. 4). The hardening function, α_{ps} is defined in terms of plastic strain trajectory ξ_v, as:

$$\alpha_{ps}=h_1/\xi_v^{h_2} \qquad (6b)$$

where h_1 and h_2 are material parameters. ξ_v denotes the trajectory of the volumetric plastic strain. Typical yield surfaces for this model are shown in Fig. 4.

Material parameters (of the model) for a marine clay found near Sabine Pass, Texas, were determined from laboratory tests (Katti 1991) and verified with available data of field tests, ("Pile Segment" 1986). Since the parameters of the model were determined and verified experimentally for Sabine clay, this clay has been used for the present study.

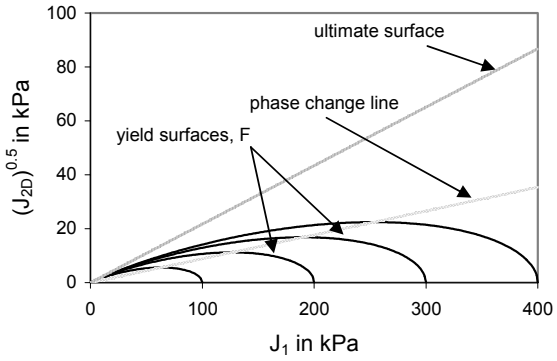

Fig. 4. Shape of yield surfaces in J_1-$\sqrt{J_{2D}}$ space.

IMPEDANCE FUNCTIONS OF THE PILE-SOIL SYSTEM

The impedance function or dynamic stiffness (K_c) includes stiffness of the system as well as the effects of inertia and damping. In the frequency domain, this is a complex quantity and can be given at a particular frequency ω by:

$$K_c=k_{st}-\omega^2 M+i\omega C \qquad (7a)$$

where k_{st} is the static (true) stiffness of the system and M is its mass. Alternatively, the complex dynamic stiffness K_c, can be evaluated in the frequency domain by applying a real load with a given amplitude, P_0, at the pile cap and noting the complex response amplitude, U_c, of the pile cap, i.e.

$$K_c=P_0/U_c \qquad (7b)$$

The dynamic stiffness of piles is a function of the loading level and frequency. In the current time domain analysis, the stiffness of the piles is evaluated as follows. For the quarter model, a harmonic lateral load of amplitude P_0, equal to 50 kN is applied at the pile cap (12.5 kN is applied on pile head for the case of single pile) and resulting displacement at the same point is noted at different frequencies of excitation. This value of load is selected to ensure that soil yielding occurs and the response becomes nonlinear. After the response stabilizes (i.e. becomes steady state), the peak amplitude of the response, U_0, and its time lag, t_l, with respect to the applied force amplitude are noted from the resulting displacement time history at the pile cap (or pile head). With these observations, the phase lag θ (in radians) and complex dynamic stiffness of the soil-pile system can be found as follows:

$$\theta=\omega t_l=2\pi f t_l \qquad (7c)$$

$$K_c=(P_0/U_0)e^{i\theta} \qquad (7d)$$

where f is frequency of excitation in Hz. Separating the dynamic stiffness, given by Eq. (7d), into real and imaginary parts, the spring constant (including effect of inertia) and damping constant can be determined.

SEISMIC EXCITATION

The control point for seismic loading is assumed at the bedrock and thus the external force in the equation of motion is found by (Clough & Penzien 1993):

$$^{t+\Delta t}R = -MP_F\, ^{t+\Delta t}\ddot{V}_b \tag{8}$$

where P_F is the pseudostatic response influence coefficient vector and $\ddot{V}_b$ is the bedrock acceleration at time $t+\Delta t$, due to vertically propagating shear waves.

COMPUTERIZATION

A FORTRAN program (3dNDPILE) was developed to perform the analysis. Finite element programming strategies suggested by Zienkiewicz (1977), Bathe (1982) and Wathugala (1990) have been incorporated in the development of the program. For nonlinear analysis, three types of criteria are used simultaneously to check the convergence of iteration, namely the displacement criteria, the out of balance load criteria and the internal energy criteria (Bathe 1982). To save space used in the storage of matrices, a skyline storage scheme (Zienkiewicz 1977) has been adopted. Special procedures have been used to ensure the robustness of the HiSS iterative solution (Wathugala 1990). These special procedures are further enhanced to deal with the case when the plasticity parameter λ (a constant of proportionality used to define the flow rule of plasticity, (Chen & Baladi 1985)) becomes negative.

Convergence of the dimensionless yield surface (F) is assumed when its absolute value becomes fairly small, i.e. when $ABS(F) < 10^{-10}$. For harmonic excitations, the step size is assumed to be $(T/20)$ where T is the time period of excitation. The algorithm developed is quite efficient and economical. A major advantage of the program is that nonlinear analyses can be performed on a normal P.C.

DATA USED IN COMPUTATION

The following data are common to all the problems considered, unless stated otherwise.

Properties of Soil

The soil is assumed to be clay at Sabine Pass, Texas. According to Desai and Wathugala (1993), its properties are as follows: Young's modulus E_s = 11.78MPa, mass density ρ_s = 1610kg/m^3, Poisson's ratio ν_s = 0.42 and material damping ratio D = 5%. The material parameters for the HiSS model are: β =0; γ = 0.047; η = 2.4; h_1 = 0.0034 and h_2 = 0.78. Details on evaluation of these parameters or how well they model the stated properties of Sabine clay can be found in Wathugala and Desai (1993).

Properties of Piles

It is assumed that the piles are made of concrete and have a square cross section with each side, d = 0.5 m. The length of the pile, l = 10 m, i.e., the pile slenderness ratio, l/d = 20. Young's modulus, mass density and Poisson's ratio for the pile are respectively:

$$E_p = 25GPa; \quad \rho_p = 2400Kg/m^3; \quad \nu_p = 0.25$$

Dynamic Loading

Seismic loading is applied as either harmonic or transient bedrock motion. Harmonic excitations consist of sinusoidal waves of unit amplitude and varying frequency. For the transient motion, an acceleration time history for the El Centro 1940 Earthquake (N-S Component), with PGA equal to 0.32g (Chopra 1995) has been used. A smoothed Fourier spectrum for this time history shows that the predominant frequency of excitation is approximately 1.83 Hz. For loading from the pile cap only harmonic excitations are considered. The response is calculated at the pile cap (or pile head) in all cases.

VERIFICATION OF MODEL AND ALGORITHM

It is important to verify the ability of the model to accurately calculate the response of the pile-soil system. This is done by performing elastic and elasto-plastic analyses and comparing the results with existing ones.

Verification for Static Loading

The pile-soil model is verified by loading an end-bearing pile laterally at the pile head. The geometry and mesh used for the pile-soil system is the same as that shown in Fig. 1a. Material properties for the soil and pile of a static case are: E_s = 20MPa; ν_s = 0.45; E_p = 20GPa and ν_p = 0.3. These properties are the same as those used by Bentley and El Naggar (2000).

The horizontal deflection of the pile head is computed for different amplitudes of applied load for the elastic, elastic-gapping and plastic-gapping cases and the results are shown in Fig. 5. The results are compared with those presented in Bentley and El Naggar (2000) (including those produced by other authors). It can be seen that for the elastic case (Fig. 5a), the results are in good agreement with those obtained by Trochanis et al. (1988) using finite element analysis, but the deflection shown by the present model is slightly less than those obtained by Bentley and El Naggar (mesh # 3), and Poulos and Davis (1980). However, Trochanis et al. (1988) considered a square pile similar to that used in the present study, while Bentley and El Naggar considered a cylindrical pile.

Figure 5b shows the pile response obtained in the present study

for the case of elasto-plastic soil compared with the response obtained Trochanis et al. (1988) and Bentley and El Naggar (2000) for elasto-plastic soil. It is noted from Fig. 5b that the results obtained from all approaches agree well for the case of plastic soil, even though different plasticity models are used (HiSS model herein and Drucker-Prager in the other studies).

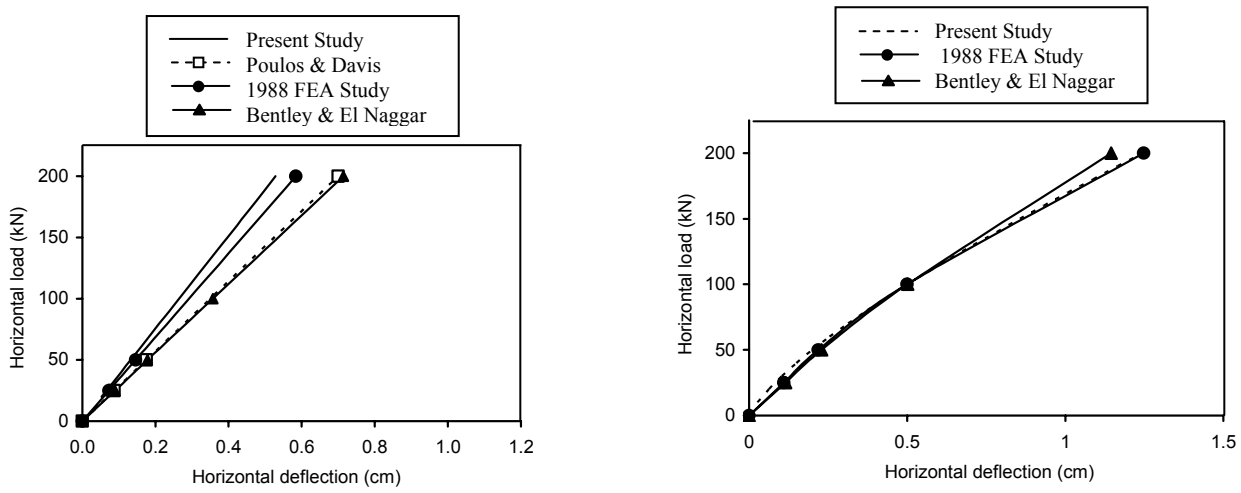

(a) Elastic Case (b) Plastic Case

Fig. 5. Verification for static loading

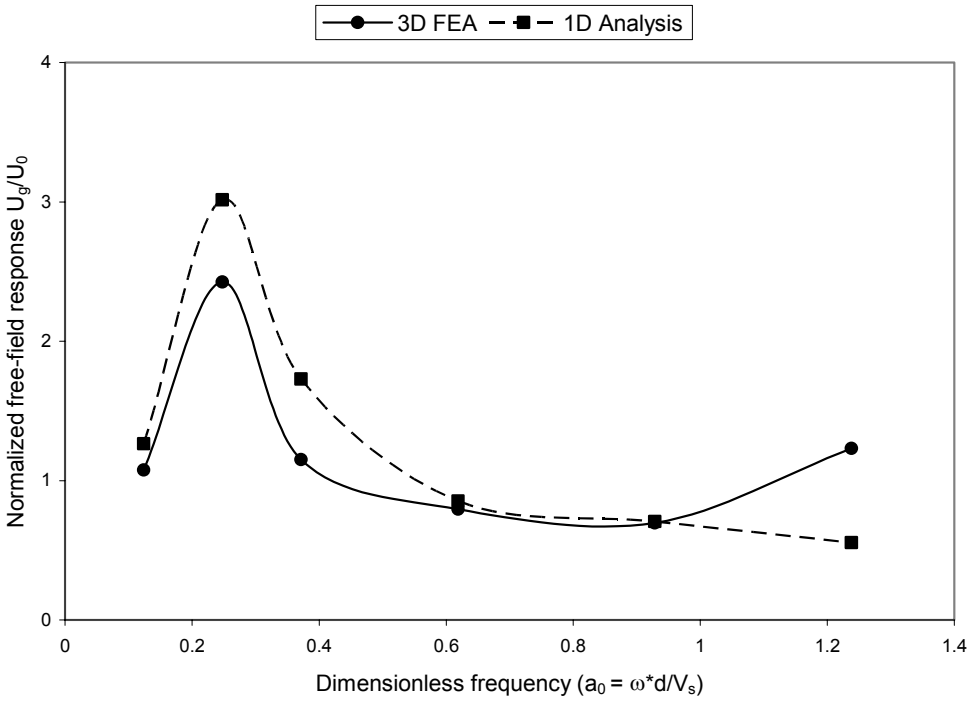

Fig. 6. Verification for free-field amplification.

Verification for Dynamic Excitations

The verification for the dynamic case included two loading schemes: seismic excitation applied as ground motion at the bedrock (to examine features of kinematic interaction) and external harmonic load applied at the pile cap (to examine features of inertial interaction). The amplitude of elastic free-field response is compared with the results from a frequency domain approach in the former case and the elastic impedance functions for pile groups are compared with a frequency domain solution in the latter case.

Free Field Response. Input bedrock motion of unit amplitude is applied and the corresponding time history of the free-field response is calculated for different excitation frequencies. The amplitude of the steady state response is noted from the free-field response time history and thus, the amplification of input motion due to soil stratum (i.e. transfer function) at different frequencies is evaluated. The amplification (transfer function) can also be calculated using a simple one-dimensional free-field response (i.e. site response) analysis in the frequency domain. Gazetas (1984) proposed the following transfer function:

$$\frac{U_g}{U_0} = \frac{1}{\cos(qL)} \quad where \quad q = \frac{2\pi f}{V_s\sqrt{(1+2iD)}} \qquad (9)$$

where U_0 and U_g are the amplitude of the input bedrock displacement and free-field ground displacement, respectively and L is height of soil stratum.

The transfer function obtained using the present 3-D FEA analysis is compared with that obtained using Eq. 9 in Fig. 6, in which a_0 is dimensionless frequency and equal to $\omega * d/V_s$. Figure 6 shows that the response obtained from the 3-D model is slightly smaller than that obtained from the 1-D model at lower and moderate frequencies (i.e. $a_0 < 0.4$). This may be attributed to higher energy dissipation in the 3-D case due to wave propagation in other directions. At higher frequencies ($0.4 < a_0 < 1.0$), plane strain conditions prevail and the response of the 3-D model approaches that of the 1-D model, as shown by the good agreement between the two approaches. Further, discrepancies may be attributed to differences in modeling material damping used (proportional damping in the 3-D model and hysteretic damping in the 1D model). It should also be noted that the value of the transfer function in the low frequency range varies between 1 and 2.5.

Impedance Functions. In the present time domain analysis complex dynamic stiffness (K_c) is found using Eq. (7d). Using Eq. (7a), it can be written as:

$$K_c = k + ik' = k + ia_0 c \qquad (10)$$

where real part $k = k_{st} - \omega^2 M$ represents stiffness (including the effect of inertia) and the imaginary part $k' = a_0 c = \omega C$ represents damping (c denotes coefficient of equivalent viscous damping). For brevity, k and c will be called stiffness and damping, respectively in subsequent discussion.

The horizontal dynamic stiffness of the pile-soil system for a single pile and 2*2 pile groups (Figs.1a-d) has been derived for the elastic case and presented in a dimensionless form in Figs. 7a-b. The dynamic stiffness is normalized with respect to the horizontal static stiffness of a single pile, $k_{xx}^{S(a_0=0)}$, multiplied by the number of piles N in the group. Subscript xx is used to denote horizontal direction while superscripts S and G are used to denote single piles and pile groups.

The results presented in Figs. 7a-b agree well with the results presented by Kanyia (1982). The trends of results for a single pile and for different pile group configurations are quite similar to those presented by Kanyia (1982). Some examples include: for closely spaced piles (s/d = 2), the group stiffness may assume negative values at higher frequencies (due to inertia effects); the stiffness curve displays peaks (Fig. 7a) for spacing (s/d = 5 and 10) (due to effects of wave interference among piles); and for close spacing (s/d = 2), damping appears to be frequency-independent (Fig. 7b). The agreement between the two sets of results verifies the model and algorithm used in the present approach. Further detailed discussion of the results is out of the scope of this paper and the reader is referred to Kanyia (1982).

EFFECTS OF NONLINEARITY ON PILE BEHAVIOR

The effects of soil nonlinearity are investigated using the numerical model that was developed. Two different sets of analysis have been performed. In the first set, the effects of soil plasticity (including work hardening) on impedance functions for a single pile as well as for 2*2 pile groups are investigated. In the second set, the effects of nonlinearity of soil on seismic response are considered.

EFFECTS OF PLASTICITY ON IMPEDANCE FUNCTIONS

The dynamic stiffness of the pile-soil system is required when calculating the response of structures supported by pile foundations to dynamic loads. The stiffness of piles is affected by the soil's nonlinear deformations that occur during extreme loading events. The dynamic stiffness of the pile-soil system has been evaluated using the linear (elastic) and nonlinear (HiSS) soil models for the cases shown in Fig 1. The results are presented in Figs. 8 to 11 in a dimensionless form, in terms of the real (stiffness k) and imaginary (damping k') parts of the dynamic stiffness (Eq. (10)).

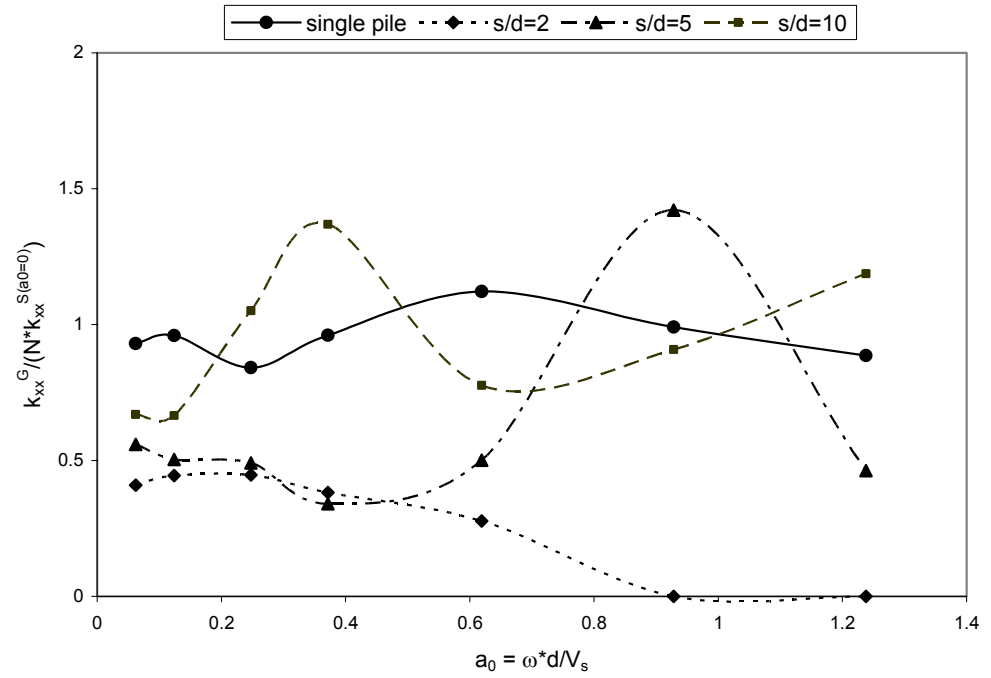

(a) Real part of dynamic stiffness

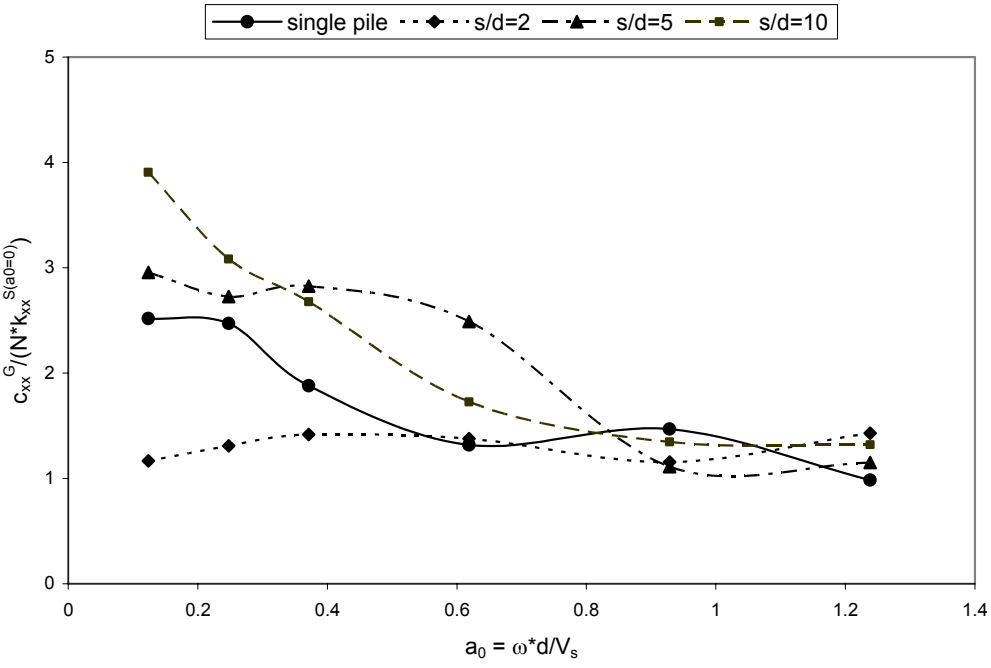

(b) Imaginary part of dynamic stiffness

Fig. 7. Verification for elastic impedance functions

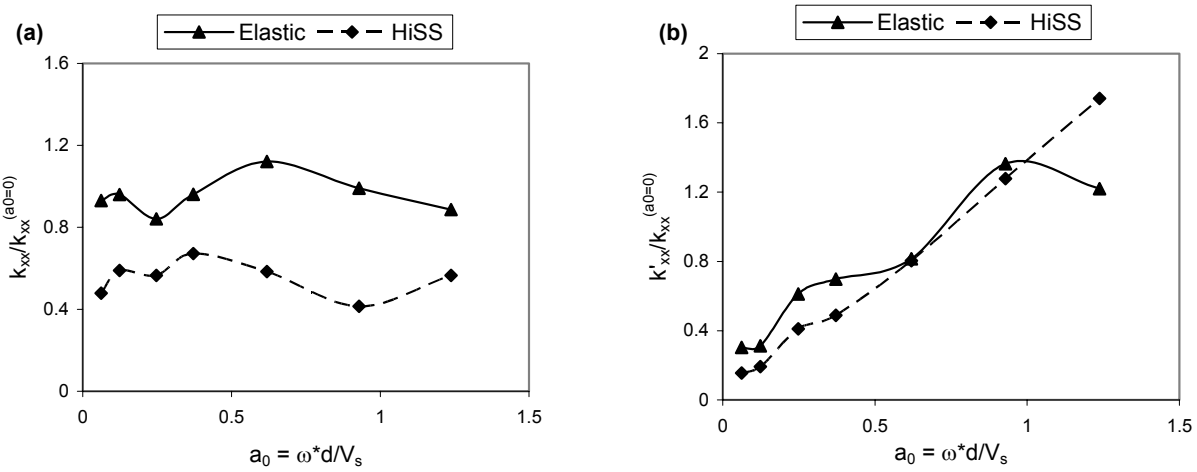

Fig. 8. Linear and nonlinear dynamic stiffness of the pile-soil system for a single pile: (a) real part (b) imaginary part.

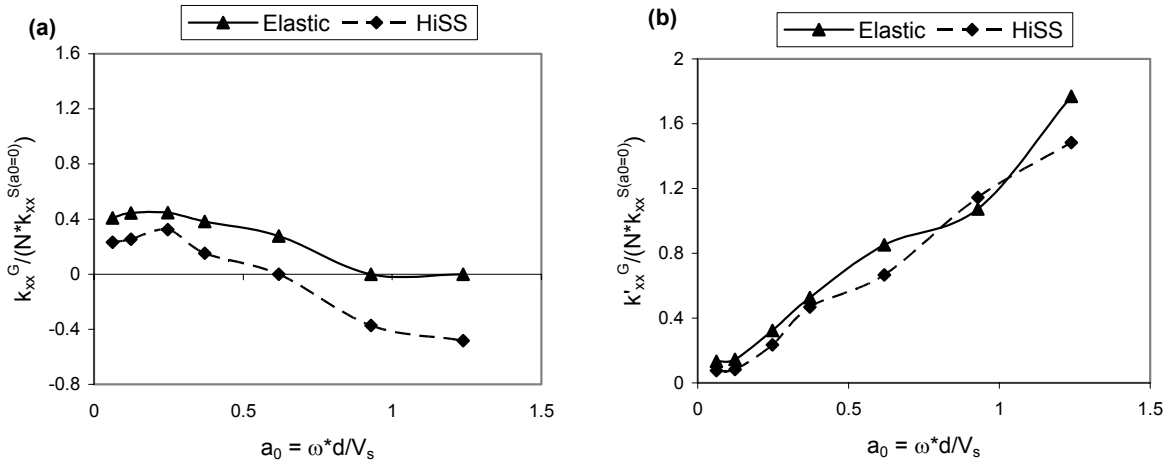

Fig. 9. Linear and nonlinear dynamic stiffness of the pile-soil system for a 2*2 pile group (s/d = 2): (a) real part (b) imaginary part.

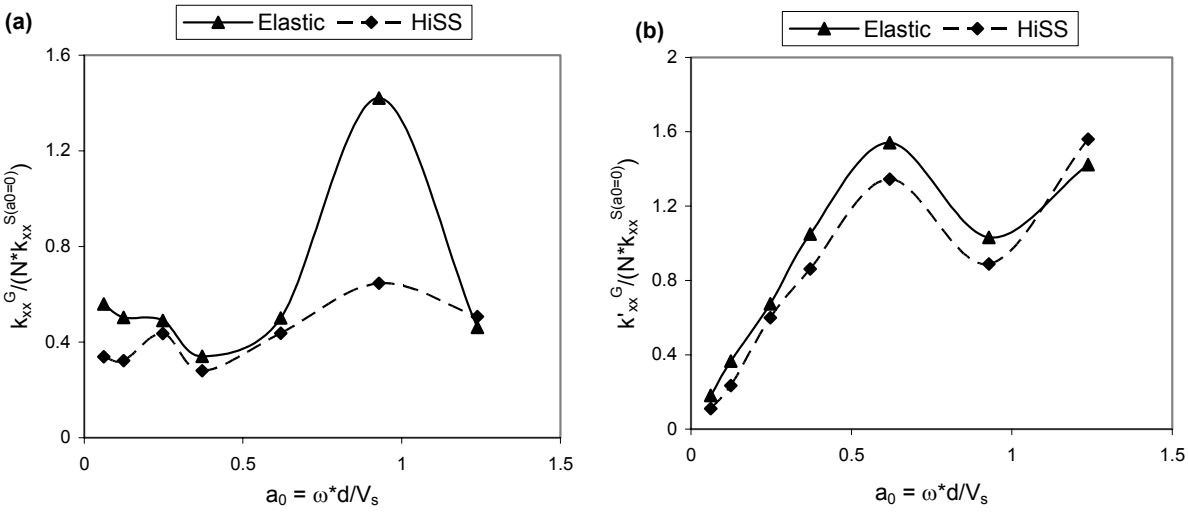

Fig. 10. Linear and nonlinear dynamic stiffness of the pile-soil system for a 2*2 pile group (s/d = 5): (a) real part (b) imaginary part.

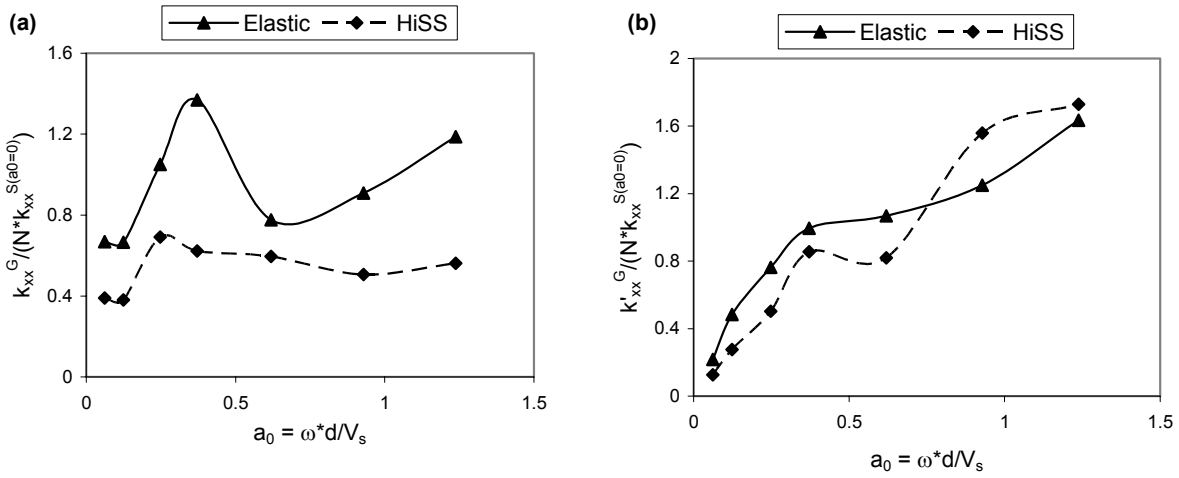

Fig. 11. Linear and nonlinear dynamic stiffness of the pile-soil system for a 2*2 pile group (s/d = 10): (a) real part (b) imaginary part.

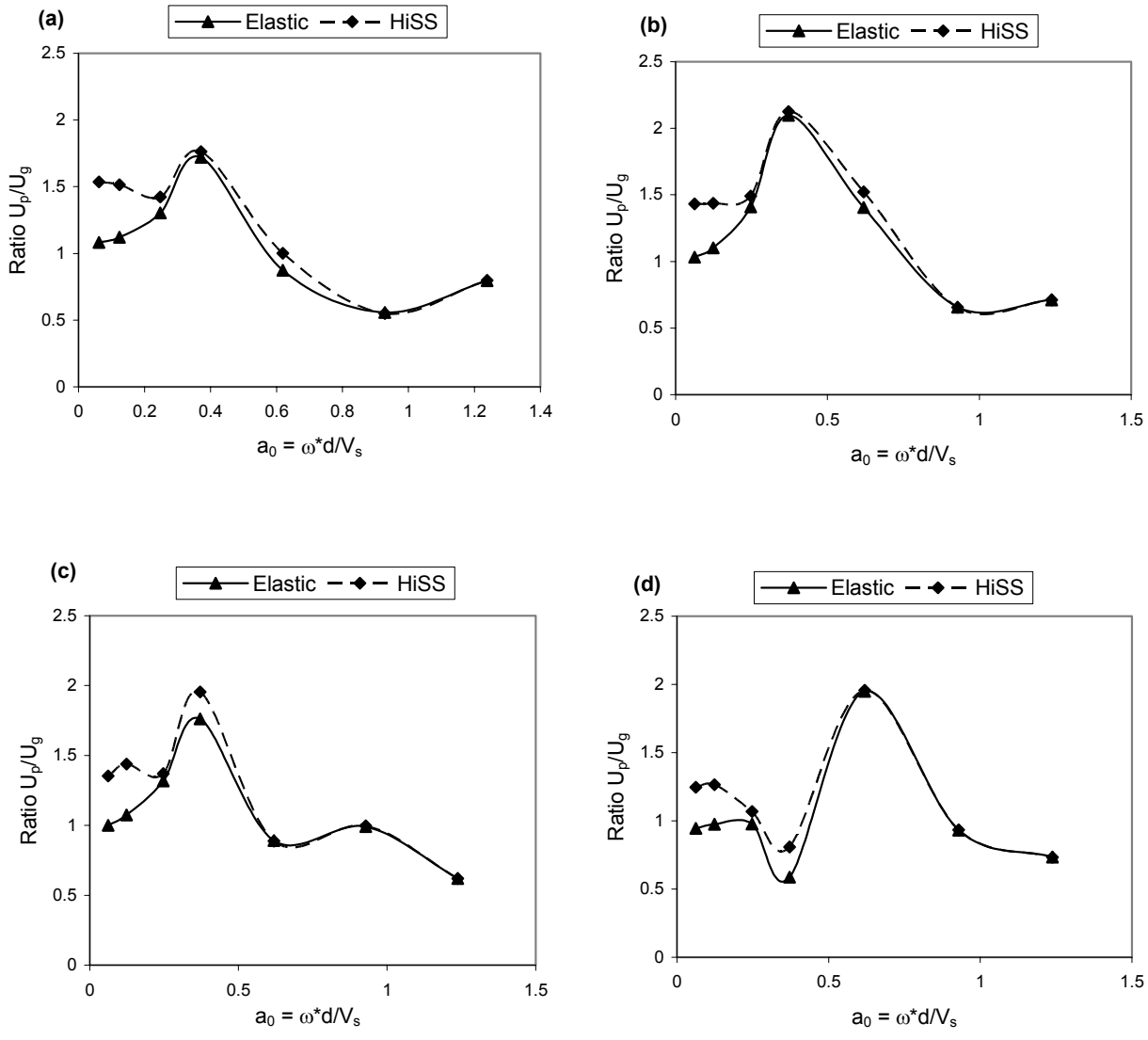

Fig. 12. Comparison of linear and nonlinear transfer functions for horizontal displacement: (a) single pile, (b) pile group (s/d = 2), (c) pile group (s/d = 5), (d) pile group (s/d = 10).

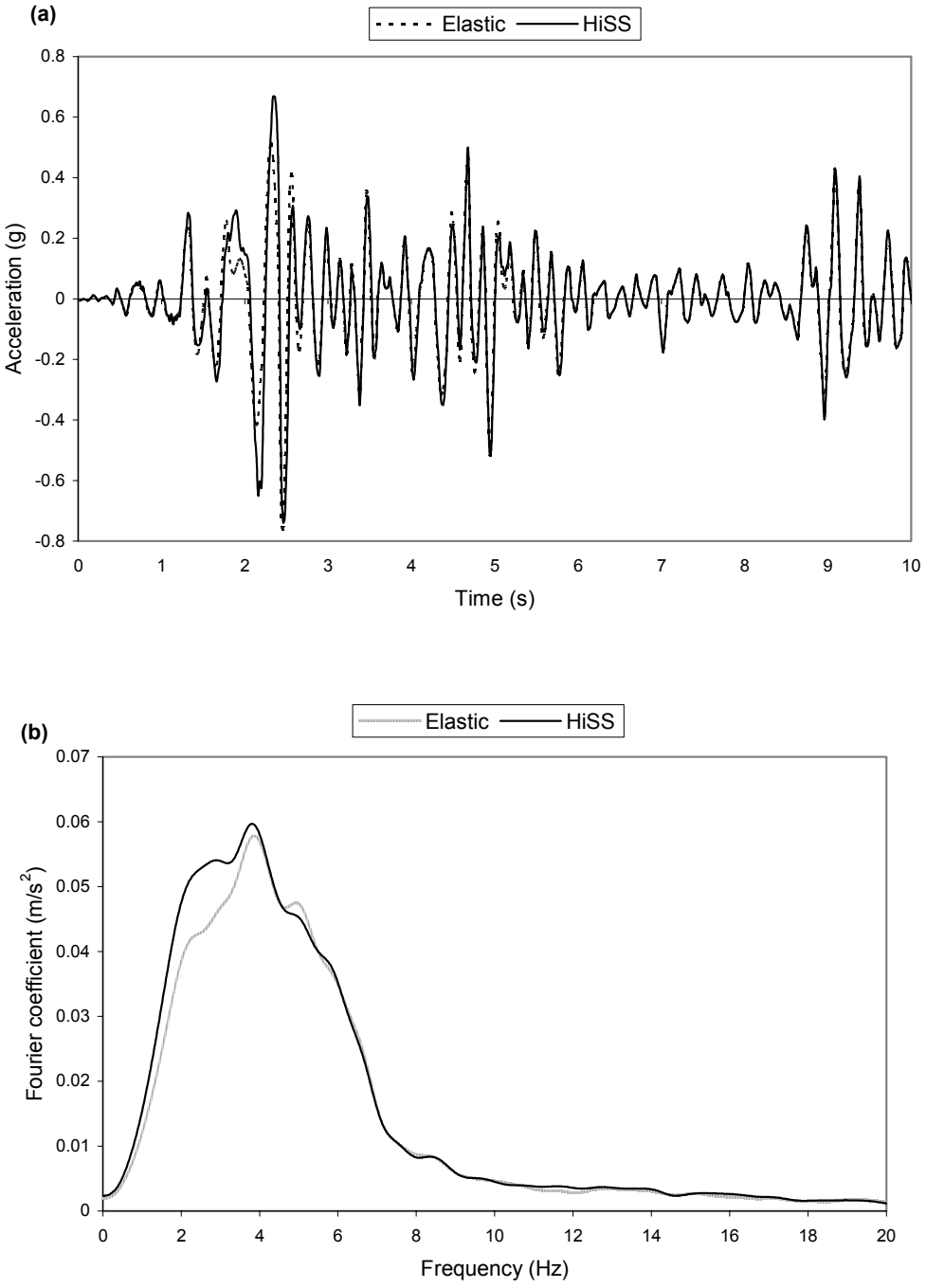

Fig. 13. Comparison of linear and nonlinear seismic response of a 2*2 pile group (s/d = 5): (a) acceleration time histories, (b) Fourier spectra.

Figure 8 shows the variation of the dynamic stiffness of a single pile with frequency. It can be noted from the figure that soil nonlinearity reduces both stiffness and damping. However, its effect is more significant on stiffness than on damping. In the nonlinear case, the damping increases almost linearly with frequency and even becomes higher than the linear case at very high frequency, probably due to higher hysteretic damping. Figure 9 shows the effects of soil plasticity on the dynamic stiffness of a 2*2 pile group with s/d = 2. It is noted that the effect of plasticity on the real part is significant, and at higher frequencies it leads to negative stiffness (high phase lag) due to a combination of a reduction of the true stiffness and an increase in inertial forces.

Figures 10 and 11 show the effects of soil nonlinearity on the impedance function of pile groups with spacing s/d = 5 and 10, respectively. It is noted from the figures that soil nonlinearity dramatically reduced the peak values of group stiffness. This is because the soil nonlinearity decreased both the stiffness of individual piles and the group effect (pile-soil-pile interaction). It also reduces damping but the effect on damping is not as important as in the case of stiffness. Nogami and Konagai (1987), Nogami et al. (1992) and El Naggar and Novak (1995) made similar observations using different models for the pile-soil system.

EFFECTS OF PLASTICITY ON SEISMIC RESPONSE

Analysis for Harmonic Excitations

The effects of soil nonlinearity on the seismic (kinematic) response of a single pile and 2*2 pile groups were investigated. The response history for the pile cap (or pile head) was derived due to an input harmonic bedrock motion of unit amplitude. The steady state response amplitude is noted from the response time history. The transfer function (or kinematic interaction factor) is then obtained by normalizing the steady state response with the elastic free-field response for the same excitation frequency.

Linear and nonlinear transfer functions are compared in Fig. 12. Figure 12a shows that the effect of nonlinearity on the transfer function for a single pile is significant for low frequencies ($a_0 <$ 0.3) but negligible for high frequencies. Similar observations can be made from Figs. 12b-d for the case of pile groups, for all cases considered here. Figure 12 also shows that the transfer function in the low frequency range varies between 1 and 2.2. This is slightly less than the transfer function for the free-field case. For seismic excitation effects of nonlinearity are significant at lower frequencies as shown in Figure 12.

Figs. 12b-d also show that unlike the case with impedance functions, the pile spacing has a small effect on the transfer function. This means that the pile-soil-pile interaction is important in inertial loading (impedance functions) but not important in kinematic loading (transfer functions).

Analysis for Transient Motion

The response at the pile cap for a 2*2 pile group with spacing s/d = 5 due to the El Centro Earthquake was calculated considering both linear and nonlinear soil models. The results for the initial 10 s from the two models are compared in Fig. 13a. Figure 13a shows that, although the maximum acceleration amplitude for the plastic case is slightly lower than that for the elastic case, most of the other peaks are higher for the plastic soil model. Bentley and El Naggar (2000) made a similar observation. Smoothed Fourier spectra of the elastic and plastic response have been derived and are shown in Fig. 13b. It is noted from Fig. 13b that the Fourier amplitudes of the response of the plastic soil model are significantly higher than those of the elastic soil model response for the low frequency range. At higher frequencies ($f >$ 6 Hz), there is hardly any difference between the two models. Therefore, the overall trend of the results is similar to that observed for harmonic excitation.

CONCLUSIONS

Effects of soil plasticity (including work hardening) on the dynamic response of pile groups are investigated. Analyses are performed for both inertial and kinematic types of loading. Comparisons of linear and nonlinear impedance functions and responses are presented.

It was found that the soil nonlinearity reduces both real and imaginary parts of the dynamic stiffness of the pile-soil system, but its effect on the real part is more significant. Nonlinearity tends to suppress the wave interference effect among piles in the group and thus reduces the stiffness significantly at excitation frequencies where the group effect is most important (i.e. near peaks on the impedance function-frequency curve). Effects of soil nonlinearity on seismic response of the pile-soil system are dependent on the frequency of excitation. At low frequencies, its effect is significant but at higher frequencies it is negligible. However, generalization of these results may require more analyses with different soil and pile parameters.

ACKNOWLEDGEMENT

The research presented here was partially supported by the Mid-America Earthquake Center under National Science Foundation Grant EEC-9701785 and the US Army Corps of Engineers. This support is gratefully acknowledged.

REFERENCES

Bathe, K.J. [1982]. *"Finite Element Procedures in Engineering Analysis"*. Prentice-Hall, Inc., Englewood Cliffs, New Jersey.

Bentley, K.J. and M.H. El Naggar [2000]. "Numerical Analysis of Kinematic Response of Single Piles", Canadian Geotechnical Journal, No. 37, pp. 1368-1382.

Cai, Y.X., P.L. Gould and C.S. Desai [2000]. "Nonlinear Analysis of 3D Seismic Interaction of Soil-Pile-Structure System and Application", Engineering Structures, No. 22(2), pp. 191-199.

Chen, W.F. and G.Y. Baladi [1985]. *"Soil Plasticity: Theory and Implementation"*. Elsevier, Amsterdam.

Chopra, A.K. [1995]. *"Dynamics of Structures"*. Prentice Hall, Inc., Upper Saddle River, New Jersey.

Clough, R.W. and J. Penzien [1993]. *"Dynamics of Structures"*. McGraw-Hill, Inc., Singapore.

Desai, C.S. and G.W. Wathugala [1993]. "Constitutive Model for Cyclic Behavior of Clays. II: Applications", Journal of Geotechnical Engineering, ASCE, No. 119(4), pp. 730-748.

Dobry, R. and G. Gazetas [1988]. "Simple Method for Dynamic Stiffness and Damping of Floating Pile Groups", Geotechnique, No. 38, pp. 557-574.

Felippa, C.A. [1975]. "Solution of Linear Equations with Skyline-Stored Symmetric Matrix", Computers and Structures, No. 5, pp. 13-29.

Gazetas, G. [1984]. "Seismic Response of End-bearing Single Piles", Soil Dynamics and Earthquake Engineering, No. 3, pp. 82-93.

Guin, J. and P.K. Banerjee [1998]. "Coupled Soil-Pile-Structure Interaction Analysis under Seismic Excitation", Journal of Structural Engineering, ASCE, No. 124(4), pp. 434-444.

Kaynia, A.M. [1982]. *"Dynamic Stiffness and Seismic Response of Pile Groups"*. Research Report R82-03, Dept. of Civil Engineering, Massachusetts Institute of Technology, Cambridge, MA.

Kaynia, A.M. and E. Kausel [1982] "Dynamic Behavior of Pile Groups", *Proc. of 2nd Int. Conf. on Numerical Methods in Offshore Piling,* Austin, Texas, pp. 509-532.

Katti, D.R. [1991]. "*Constitutive Modeling and Testing of Saturated Marine Clay"*. PhD dissertation, Dept. of Civil Eng. and Eng. Mechanics, Univ. of Arizona, Tucson, Arizona.

Kramer, S.L. [1996]. *"Geotechnical Earthquake Engineering"*. Prentice Hall, Inc., Upper Saddle River, New Jersey.

Maheshwari, B.K., K.Z. Truman, P.L. Gould and M.H. El Naggar [2002]. "Three-dimensional Nonlinear Seismic Analysis of Single Piles using FEM: Effects of Plasticity of Soil", In review for International Journal of Geomechanics.

Makris, N. and G. Gazetas [1992]. "Dynamic Pile-Soil-Pile Interaction. Part II: Lateral and Seismic Response", Earthquake Engineering and Structural Dynamics, No. 21, pp. 145-162.

Nogami, T. and K. Konagai [1986]. "Time Domain Axial Response of Dynamically Loaded Single Piles", Journal of Engineering Mechanics, ASCE, No. 112(11), pp. 1241-1252.

Nogami, T. and K. Konagai [1987]. "Dynamic Response of Vertically Loaded Nonlinear Pile Foundations", Journal of Geotechnical Engineering, ASCE, No. 113(2), pp. 147-160.

Nogami, T., and K. Konagai [1988]. "Time Domain Flexural Response of Dynamically Loaded Single Piles", Journal of Engineering Mechanics, ASCE, No. 114(9), pp. 1512-1525.

Nogami, T., J. Otani, K. Konagai, and H.L. Chen [1992]. "Nonlinear Soil-Pile Interaction Model for Dynamic Lateral Motion", Journal of Geotechnical Engineering, ASCE, No. 118(1), pp. 89-106.

Novak, M., T. Nogami and F. Aboul-Ella [1978]. "Dynamic Soil Reaction for Plane Strain Case", Technical note, Journal of Engineering Mechanics, ASCE, No. 104(4), pp. 953-956.

Novak, M. and H. Mitwally [1988]. "Transmitting Boundary for Axisymmetrical Dilation Problems", Journal of Engineering Mechanics, ASCE, No. 114(1), pp. 181-187.

Pile Segment Tests-Sabine Pass [1986]. *"Some Aspects of the Fundamental Behavior of Axially Loaded Piles in Clay Soils"*. ETC Report No. 85-007, Earth Technology Corp., Houston, Texas.

Poulos, H.G. and E.H. Davis [1980]. *"Pile Foundation Analysis and Design"*. John Wiley & Sons, New York.

Sen, R., T.G. Davis and P.K. Banerjee [1985]. "Dynamic Analysis of Piles and Pile Groups Embedded in Homogenous Soils", Earthquake Engineering and Structural Dynamics, No. 13(1), pp. 53-65.

Trochanis, A.M., J. Bielak and P. Christiano [1988]. *"A three-dimensional Nonlinear Study of Piles Leading to the Development of a Simplified Model"*. Technical Report of Research Sponsored by NSF Grant ECE-86/1060 Carnegie Mellon University, Washington, D.C.

Wathugala, G.W. [1990]. *"Finite Element Dynamic Analysis of Nonlinear Porous Media with Applications to Piles in Saturated Clays"*. Ph.D. dissertation, Dept. of Civil Eng. and Eng. Mechanics, Univ. of Arizona, Tucson, Arizona.

Wathugala, G.W. and C.S. Desai [1993]. "Constitutive Model for Cyclic Behavior of Clays. I: Theory", Journal of Geotechnical Engineering, ASCE, No. 119(4), pp. 714-729.

Wolf, J.P. [1985]. *"Dynamic Soil-Structure-Interaction"*. Prentice-Hall, Inc., Englewood Cliffs, New Jersey.

Wu, G. and W.D.L. Finn [1997]. "Dynamic Nonlinear Analysis of Pile Foundations using Finite Element Method in the Time Domain, Canadian Geotechnical Journal, No. 34, pp. 44-52.

Zienkiewicz, O.C. [1977]. *"The finite element method, 3rd Edition"*. McGraw-Hill Book Company, U.K.